

Laser induced temperature effects in multi-walled carbon nanotubes probed by Raman spectroscopy

Jaroslav Judek¹, Cezariusz Jastrzebski¹, Artur Malolepszy², Marta Mazurkiewicz², Leszek Stobinski^{2,3}, and Mariusz Zdrojek^{*1}

¹Faculty of Physics, Warsaw University of Technology, Koszykowa 75, Warsaw 00-662, Poland

²Faculty of Materials Science and Engineering, Warsaw University of Technology, Woloska 141, Warsaw 02-507, Poland

³Polish Academy of Sciences, Institute of Physical Chemistry, Kasprzaka 44/52, Warsaw 01-224, Poland

Received 3 October 2011, revised 2 November 2011, accepted 3 November 2011

Published online 24 November 2011

Keywords carbon nanotubes, Raman spectroscopy, temperature effects

* Corresponding author: e-mail zdrojek@if.pw.edu.pl, Phone: +48-22-2347170, Fax: +48-22-2345447

We examined the influence of continuous laser irradiation on as-prepared and oxidized multi-walled carbon nanotubes (MWCNTs) on the basis of Raman scattering. Differences between Raman spectra for both types of nanotube samples are shown. We evaluate the influence of the laser power density (LPD) on two main Raman modes (D and G) based on the

position of the peaks, widths, and the relative intensity I_D/I_G ratio. Impurities and their interaction with nanotubes are crucial for interpretation of the measured effects. Oxidation, as well as the irradiation process, improves purity of samples. No structural changes of the tubes are observed. The Raman signal decrease is likely to originate from nanotube loss.

© 2011 WILEY-VCH Verlag GmbH & Co. KGaA, Weinheim

1 Introduction Raman spectroscopy has proven to be convenient technique to characterize structural, thermal, and electronic properties of carbon nanostructures [1]. However, the laser irradiation can lead to a significant sample heating during the measurement process. It has been shown that higher local temperature increases the carbon–carbon interatomic distance thus shifting the Raman peaks to lower frequencies [2–4]. This effect is especially pronounced in heavily defected or disordered tubes due to the enhanced increase in carbon–carbon distance [5]. Moreover, in contaminated carbon nanotubes, the local temperature stemmed from laser irradiation might be higher due to increased heating rate originating from lower thermal conductivity and higher absorption of the contaminants [6]. In addition, due to the laser induced temperature raise nanotubes can undergo structural changes like purification, self-healing, selective destruction, or transformation to C₆₀ molecules [7–12]. Heating can also lead to the change of molecular doping (e.g., desorption of O₂, H₂O) implying changes in Raman spectra of sp² carbons [13].

The temperature effects in carbon nanotubes probed by Raman spectroscopy have been intensively investigated in the past several years [2–6]. However, laser induced heating

effects seen in Raman spectra have been mainly investigated in single-walled carbon nanotubes (SWCNTs) [7–12], both as-grown and functionalized. So far, only as-prepared multi-walled carbon nanotubes (MWCNTs) films were investigated [14, 15]. Here, we study the influence of continuous laser irradiation on as-prepared and oxidized MWCNT on the basis of Raman scattering. To the best of our knowledge, this has not been reported yet. We investigate the influence of the laser power density (LPD) on two main Raman modes (D and G) looking at the position of the peaks, their widths, and the integrated I_D/I_G ratio.

Heating effects in carbon nanotubes may find application in the standards for optical power measurements devices [16], which are essential for laser systems used in industry, communications, and other technologies. In addition, it has been demonstrated that MWCNTs coupled with laser irradiation can be used to enhance treatment of cancer cells [17]. Our results on heating effects in carbon nanotubes may give additional information to be used in these applications.

2 Samples and experimental setup Multi-walled carbon nanotubes (93% weight purity) were grown using the CVD technique (CNT Co., LTD., Korea), with diameter

ranging from 10 to 40 nm and length up to 25 μm. Part of MWCNTs was purified with concentrated nitric acid under reflux for 50 h in 120 °C. Next, all tubes were washed with water in order to reach chemical neutrality, and then dried. The details of the oxidation process are published elsewhere [18]. For the measurements agglomerated MWCNTs (powder form) are deposited on Si/SiO₂ wafer.

Raman spectra were acquired by means of standard microRaman spectroscopy technique [19] using the triple grating Dilor XY-800 spectrometer having resolution 1–2 cm⁻¹ for argon laser line: 514 nm. The spectra of the D and the G band were collected in one spectral window. Spectrometer was calibrated with the Argon plasma lines. All measurements have been performed at ambient pressure and room temperature. Standard accumulation time was 2 × 60 s. Calibrated laser power on the sample was swept from 0.7 up to 20 mW. The laser spot focused with the 50× objective has a diameter ~5 μm, thus the power density varies from 3.5 to 100 kW/cm².

3 Results and discussion First we present the Raman spectra of as-prepared and oxidized MWCNTs. At this point, we used the lowest LPD – 3.5 kW/cm² in order to avoid temperature effects. A typical Raman spectrum of both nanotube samples is shown in Fig. 1. The Raman spectra consist of two main peaks: G, D, and less pronounced D' peak. The G band located at ~1580 cm⁻¹ is related to E_{2g} graphite mode, indicating C–C stretching vibrations. Two disorder-induced bands are observed – D located at about 1350 cm⁻¹ and D' at about 1620 cm⁻¹ [20]. For simplicity we focus on analysis of two main peaks (G and D). The intensity ratio of the G and D peaks (*I_D/I_G*), frequently used in this work, refers to the ratio of integrated area under the respective curve.

As seen in Fig. 1, oxidation changes significantly the Raman spectrum of carbon nanotubes. The positions of the D and G mode shift from 1346 to 1355 cm⁻¹, and from 1572 to

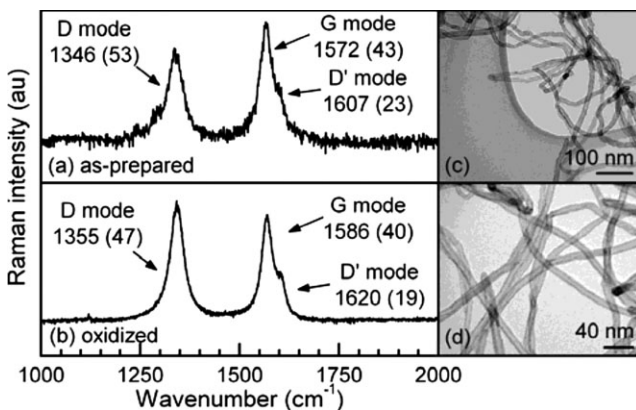


Figure 1 Raman spectra showing as-prepared (a) and oxidized (b) multi-walled carbon nanotubes. TEM pictures showing as-prepared (c) and oxidized (d) MWCNTs. In brackets – the full width at the half maximum (FWHM). Both Raman spectra were recorded with 514 nm laser line and with the lowest 3.5 kW/cm² laser power.

1586 cm⁻¹, respectively. The full width at the half maximum of the D and G modes' is also changed: from 53 to 47 cm⁻¹ and from 43 to 40 cm⁻¹, respectively. The *I_D/I_G* intensity ratio rises from 0.75 up to 1.44 for oxidized tubes. Higher noise intensity on the Fig. 1a is connected with lower signal intensity from the as-prepared samples.

Wavenumbers of both Raman modes for oxidized nanotubes have typical, literature values [1]. However, G and D mode positions for as-prepared MWCNTs are unambiguously downshifted. These shifts might be related to some sort of strain deformation, mode softening, and/or higher heating rate due to the higher amount of the amorphous carbon and other contaminants in the vicinity of the tubes. Purification can remove part of the impurities restoring disturbed phonon frequencies. The increase in the *I_D/I_G* ratio is most likely attributed to the increase in defects concentration related to the oxidation of MWCNTs [18]. According to Ferrari [21] higher disorder reflected by the *I_D/I_G* ratio should imply larger peak widths. The decrease in the FWHM of D and G mode and the increase in the *I_D/I_G* ratio are rather an unexpected result and may also indicate that oxidized tubes are in fact better quality than the as-prepared ones.

We now turn our attention to the laser induced heating effect in MWCNTs. Figure 2 shows changes of the D and G modes wavenumbers as a function of laser illumination intensity for as-prepared and oxidized carbon nanotubes. First the laser power was increased up to 100 kW/cm² and then, subsequently back to 3.5 kW/cm². For the laser power increase (up to 100 kW/cm²), both main peaks (G and D) position for as-prepared nanotubes changes less than 3 cm⁻¹. This suggests, rather little effect of the laser irradiation. However, one needs to remember that the wavenumber shift

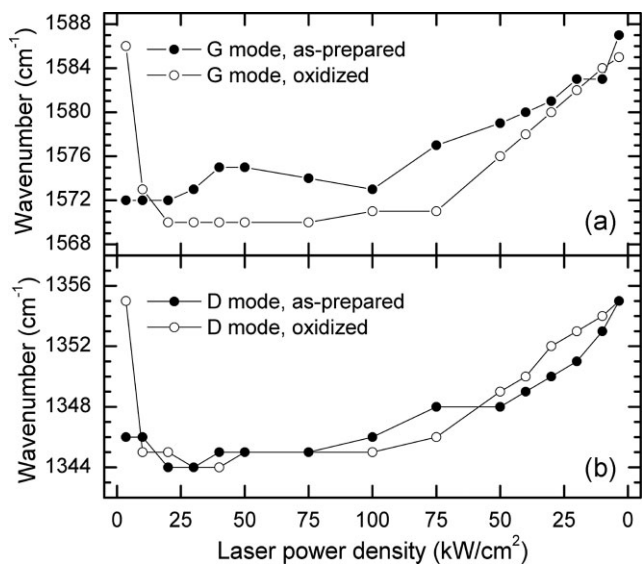


Figure 2 The G mode (a) and D mode (b) position versus laser power density for as-prepared (full circles) and oxidized (open circles) MWCNTs. The laser power density was first increased from 3.5 to 100 kW/cm² and subsequently decreased back to 3.5 kW/cm².

reflects local temperature of the sample and above certain temperature the shift can saturate. The G and D modes for oxidized nanotubes show different behavior: at the beginning for the lowest laser power we observe drastic peak downshift ($\sim 10 \text{ cm}^{-1}$), then it stabilizes for higher powers (up to 100 kW/cm^2).

After maximum laser power (100 kW/cm^2) is reached, we continue with the laser irradiation but decreasing the laser power. Surprisingly, the D and G modes quite linearly upshift for both nanotube samples. The G mode's wavenumber of as-prepared MWCNTs changes from 1573 to 1587 cm^{-1} , the D mode's wavenumber changes from 1346 to 1355 cm^{-1} .

Above results lead to the following conclusions. At the beginning the samples are heating proportionally to their purity (for details see Ref. [6]). Results for as-prepared samples (Fig. 2) show that the maximal shift value even for the lowest LPD has been already reached. Oxidation implies, e.g., lower amorphous carbon contamination thus lower heating rate and no wavenumber shift for the lowest LPD. Intense laser radiation has similar impact on studied samples as oxidation. It purifies tubes thus lowering their heating rate. The observed linear upshift is attributed to shortening of the C–C distances as the nanotube is cooling down, what was observed frequently for SWCNTs [2–4]. The origin of the lower wavenumber limit attributed to the highest temperature will be discussed later. We note that our experiments have been conducted in ambient pressure and room temperature, therefore the effect of heating induced change in molecular doping could be also present in our spectra. However, we were not able to distinguish the impact of such doping, because this would require an experiment in strictly controlled environment (e.g., vacuum cryostat).

The analysis of the other features of the D and G bands also provides interesting information on the laser heating effects in nanotubes. Here, we look at the peaks width and the relative integrated peak intensity. Those parameters *versus* laser power are shown in Fig. 3. After whole irradiation process the values of FWHM of both modes for both types of samples are decreased. The G mode width decreases by 8 cm^{-1} for as-prepared nanotubes and by 9 cm^{-1} for oxidized tubes (Fig. 3a). The width of the D mode decreases from 55 to 43 cm^{-1} for as-prepared tubes and for oxidized nanotubes it changes from 46 to 35 cm^{-1} (see Fig. 3b). In general, the decrease in FWHM of D and G mode is related to prolongation of the lifetime of phonons, e.g., due to lower defects concentration or lower temperature, it could also be related to homogeneity of the sample. The local maximum for most intense laser power (100 kW/cm^2) is related to the decreasing in the phonon lifetime at higher temperatures.

The I_D/I_G integrated intensity ratio shown in Fig. 3c has a tendency to slight decrease as the laser power is increased. It changes from 0.75 to 0.56 for as-prepared nanotubes and from 1.45 to 1.21 for oxidized nanotubes. Almost constant I_D/I_G ratio and decrease of peaks width further confirm higher quality of the samples after irradiation process. Importantly, such irreversible behavior is observed only for

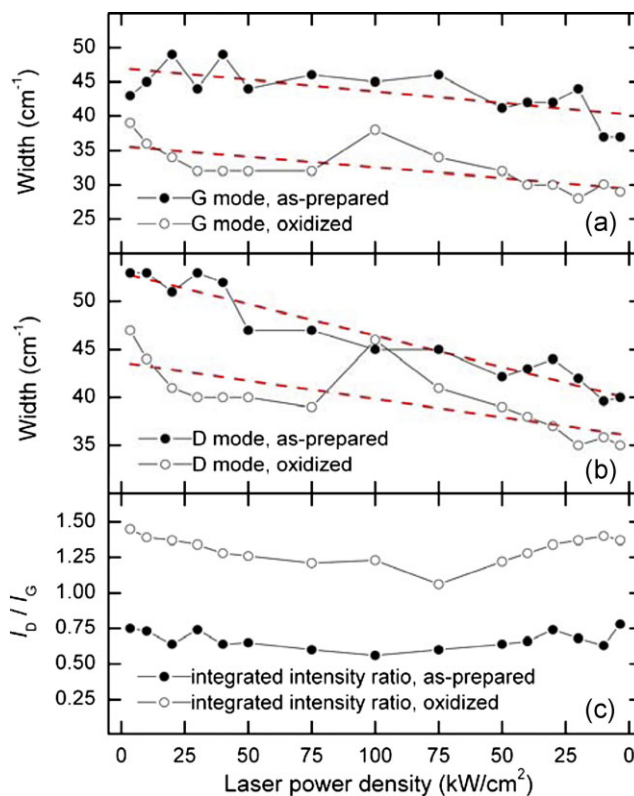


Figure 3 (online color at: www.pss-a.com) The G mode width (a), D mode width (b), and integrated intensity ratio (c) *versus* laser power density for as-prepared (full circles) and oxidized (open circles) MWCNTs. The red bar-lines stand for the linear fit of experimental data. (c) Integrated intensity ratio of the D and G band as a function of laser power density.

the first power sweep cycle, thus supporting our claim that laser irradiation purifies carbon nanotubes. Subsequent power sweeps cycles are reversible, particularly, the peak positions and their widths for the lowest LPD are constant. It means that no further purification with LPDs below 100 kW/cm^2 is possible and sample is stable under laser irradiation.

Finally, we compare the intensity of the G band before and after the power sweep cycle. The integrated intensity of the G band was significantly decreased to about one third of its initial value for both as-prepared and oxidized nanotubes. However, as it is seen in Fig. 3c, the I_D/I_G ratio is not changed. Therefore it contradicts any expectation of structural changes in nanotubes (destruction) and more likely suggests nanotube expelling. MWCNTs can be blown away by evaporating contaminants surrounding them.

Summarizing, we have shown that controlled continuous laser irradiation on as-prepared and oxidized MWCNTs induce heating effects which lead for instance to improvement of samples purity. In order to prove this we investigated the change of two main Raman MWCNTs modes position, their widths and the integrated I_D/I_G ratio.

Acknowledgements This work was supported by the Polish Council for Science through the Development Grant for the years

2008–2011 (NR 15-0011-04/2008) and 2008-2013 (KB/72/13447/IT1-B/U/08). MZ thank for the support from FNP Homing Plus project.

References

- [1] A. Jorio, M. Dresselhaus, R. Saito, and G. F. Dresselhaus, *Raman Spectroscopy in Graphene Related Systems* (Wiley-VCH, Berlin, Weinheim, New York, 2011).
- [2] H. D. Li, K. T. Yue, Z. L. Lian, Y. Zhan, L. X. Zhou, S. L. Zhang, Z. J. Shi, Z. N. Gu, B. B. Liu, R. S. Yang, H. B. Yang, G. T. Zou, Y. Zhang, and S. Iijima, *Appl. Phys. Lett.* **76**, 2053 (2000).
- [3] N. R. Raravikar, P. Koblinski, A. M. Rao, M. S. Dresselhaus, L. S. Schadler, and P. M. Ajayan, *Phys. Rev. B* **66**, 235424 (2002).
- [4] L. Ci, Z. Zhou, L. Song, X. Yan, D. Liu, H. Yuan, Y. Gao, J. Wang, L. Liu, W. Zhou, G. Wang, and S. Xie, *Appl. Phys. Lett.* **82**, 3098 (2003).
- [5] F. Huang, K. Yue, P. Tan, S. Zhang, Z. Shi, X. Zhou, and Z. Gu, *J. Appl. Phys.* **84**, 4022 (1998).
- [6] S. V. Terekhov, E. D. Obraztsova, A. S. Lobach, and V. I. Konov, *Appl. Phys. A* **74**, 393 (2002).
- [7] L. Zhang, H. Li, K. Yue, and S. Zhang, *Phys. Rev. B* **65**, 073401 (2002).
- [8] P. Corio, P. S. Santos, M. A. Pimenta, and M. S. Dresselhaus, *Chem. Phys. Lett.* **360**, 557 (2002).
- [9] M. Kalbac, L. Kavan, L. Juha, S. Civis, M. Zúkalová, M. Bittner, P. Kubat, V. Vorlíček, and L. Dunsch, *Carbon* **43**, 1610 (2005).
- [10] H. Huang, R. Maruyama, K. Noda, H. Kajiura, and K. Kadono, *J. Phys. Chem. B* **110**, 7316 (2006).
- [11] P. Puech, F. Puccianti, R. Bacsa, C. Arrondo, V. Paillard, A. Bassil, M. Monthieux, E. Flahaut, F. Bardé, and W. Bacsa, *Phys. Rev. B* **76**, 054118 (2007).
- [12] D. Olevik, A. V. Soldatov, M. Dossot, B. Vigolo, B. Humbert, and E. McRae, *Phys. Status Solidi B* **245**, 2212 (2008).
- [13] Z. H. Ni, H. M. Wang, Z. Q. Luo, Y. Y. Wang, T. Yu, Y. H. Wu, and Z. X. Shen, *J. Raman Spectrosc.* **41**, 479 (2010).
- [14] A. Kumar, F. Singh, P. M. Koinkar, D. K. Avasthi, J. C. Pivin, and M. A. More, *Thin Solid Films* **517**, 4322 (2009).
- [15] T. Nakamiya, F. Mitsugi, K. Semba, R. Kozai, T. Ikegami, Y. Iwasaki, Y. Sonda, and R. Tsuda, *Thin Solid Films* **517**, 3854 (2010).
- [16] J. H. Lehman, C. Engtrakul, T. Gennett, and A. C. Dillon, *Appl. Optics* **44**, 483 (2005).
- [17] J. W. Fisher, S. Sarkar, C. F. Buchanan, C. S. Szot, J. Whitney, H. C. Hatcher, S. V. Torti, C. G. Rylander, and M. N. Rylander, *Cancer Res.* **70**, 9855 (2010).
- [18] L. Stobinski, B. Lesiak, L. Kövér, J. Tóth, S. Biniak, G. Trykowski, and J. Judek, *J. Alloys Compd.* **501**, 77 (2010).
- [19] J. Judek, D. Brunel, T. Mélin, M. Marczak, M. Zdrojek, W. Gebicki, and L. Adamowicz, *Phys. Status Solidi C* **6**, 2056 (2009).
- [20] C. Thomsen and S. Reich, *Phys. Rev. Lett.* **85**, 5214 (2000).
- [21] A. C. Ferrari, *Solid State Commun.* **143**, 47 (2007).